Design of Multimode Horn Feed for Parallel Plate Waveguide-Based Offset Dual-Reflector Antenna

Citation for the original published paper (version of record):

Thi-Kim-Ngan Nguyen, Vilenskiy, A., Gonzalez-Ovejero, D. et al (2025). Design of Multimode Horn Feed for Parallel Plate Waveguide-Based Offset Dual-Reflector Antenna. 2025 55TH EUROPEAN MICROWAVE CONFERENCE, EUMC: 965-968

(article starts on next page)

Design of Multimode Horn Feed for Parallel Plate Waveguide-Based Offset Dual-Reflector Antenna

Thi-Kim-Ngan Nguyen[1], Artem R. Vilenskiy[2], David González-Ovejero[1], Ronan Sauleau[1], Marianna V. Ivashina[3]
[1]Univ Rennes, CNRS IETR UMR 6164, France
[2]Microwave Team, Emerging Technologies Research Center, XPANCEO, UAE
[3]Antenna Systems Group, Dept. of Electrical Engineering, Chalmers University of Technology, Sweden
{thi-kim-ngan.nguyen, david.gonzalez-ovejero, ronan.sauleau}@univ-rennes.fr, artem.vilenskiy@xpanceo.com,
marianna.ivashina@chalmers.se

***Abstract*— This paper presents the design of a W-band multimode horn feed (MHF) to illuminate an offset dual-reflector system in a parallel-plate waveguide (PPW), aiming to improve the antenna efficiency by achieving nearly uniform aperture illumination. While conventional horns typically achieve $\sim 80\%$ aperture efficiency in classical reflector systems, an open question is how closely multimode horn feeds can approach the theoretical efficiency limit in PPW-based architectures. The proposed MHF incorporates a horizontal stepped waveguide structure to excite higher-order modes, each with a specific complex coefficient, thereby producing a sub-reflector illumination pattern that closely approximates the ideal secant profile. The MHF design has been explored for both single-polarized and dual-polarized configurations, achieving a taper efficiency of 97% for the reflector system in PPW. The design trade-offs for achieving high taper efficiency and minimal spillover loss, while addressing challenges such as multiple sidewall reflections and phase aberrations in closed metallic structures, are also discussed.**

***Keywords*— Reflector antenna, mutimode horn, parallel-plate waveguide (PPW), mm-wave, sub-THz antennas.**

I. INTRODUCTION

Next-generation wireless communication systems are expected to provide higher data rates than present-day solutions to meet the growing demand for fast and reliable information access. This advancement calls for the development of innovative antennas operating above 100 GHz [1]–[3]. To compensate for increased material dissipation and free-space path loss at mm-wave and sub-THz frequencies, these antennas require higher gain (typically above 30 dBi). In this regard, low-profile antennas with quasi-optical beamformers integrated into parallel-plate waveguides (PPWs) are particularly promising due to their high directivity, high radiation efficiency, multi-beam capabilities, and scalable, modular implementation [4]. However, electromagnetic design and optimization can be challenging due to a complex, multi-scale structure (with electrically large overall dimensions and fine geometrical features).

The present work builds upon the previous study in [5], which presented a low-profile, broadband, dual-linearly polarized offset dual-reflector antenna at W-band (75–110 GHz). This solution offers an advantage over most conventional PPW quasi-optical beamformers, which are typically limited to single polarization, by leveraging dual-mode excitation (quasi-TEM and quasi-TE_1 modes) in an overmoded PPW. However, this antenna exhibits moderate aperture efficiency (approximately 30%). Enhancing the aperture field uniformity of the offset dual-reflector system is a promising strategy for improving overall antenna efficiency. A key approach to achieving this is tailoring the horn feed to produce the desired feed pattern. Pattern shaping of horn antennas have been extensively studied to enhance key performance metrics, including cross-polarization, aperture efficiency, and sidelobe levels [6], [7].

Our work aims to design a multimode horn feed to illuminate the offset dual-reflector system in the PPW. The goal is to obtain a feed pattern similar to an ideal secant distribution, which would produce a reflector antenna with a uniformly illuminated aperture and minimal spillover loss [8]. The design process begins with the analysis and synthesis of a single-polarized multimode horn in PPW, as discussed in Section II, and is later extended to a dual-linearly polarized configuration in Section III. The performance of the antenna system is evaluated through a comparative analysis with a system utilizing the original horn. Finally, conclusions are drawn in Section IV.

II. SINGLE-POLARIZED MULTIMODE HORN FEED

The considered offset dual-reflector system illuminated by a multimode horn feed (MHF) in the PPW is shown in Fig. 1 (a), with the focal ratio of $F_m/D_m = 0.5$, assuming the sub-reflector is nearly in the far-field region of the feed horn. First, we discuss the design of a single-polarized MHF in the PPW, as illustrated in Fig. 1 (b). The height of the PPW, denoted as H_0, is set to $0.4\lambda_0$, where λ_0 is the free-space wavelength at the central design frequency f_0 = 90 GHz. This configuration ensures that only the fundamental TEM mode propagates in the PPW.

The detailed schematic of the proposed MHF is shown in Fig. 2. The MHF is excited by the fundamental TE_{10} mode of a standard rectangular waveguide (WG), with multiple WG steps introduced to generate higher-order modes, each with a specific complex coefficient. A tapered section with a flared

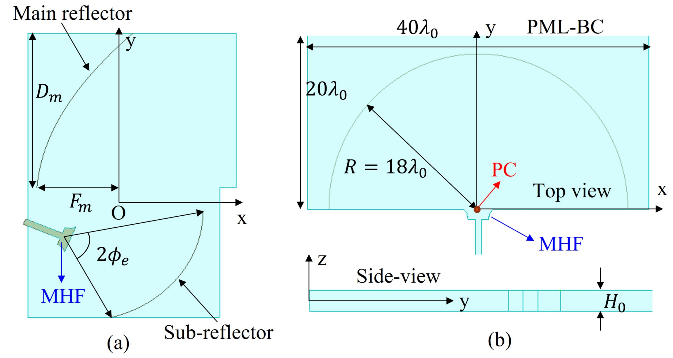

Fig. 1. (a) Geometry of offset dual-reflector system illuminated by MHF in PPW. (b) Configuration of MHF in PPW. Note: the arc radius represents the distance from the MHF phase center (PC) to the sub-reflector tip.

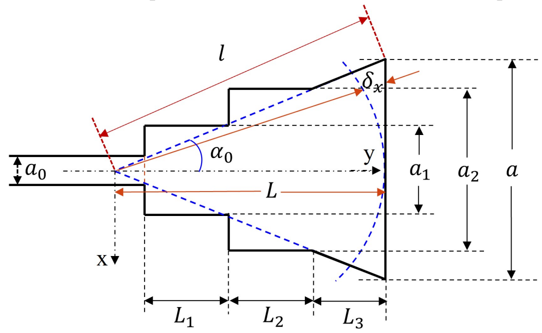

Fig. 2. Schematic of the proposed MHF.

angle α_0 is incorporated to facilitate impedance matching. For the given H_0, only TE_{m0} (to y) modes propagate in the horn with no variations along the z-axis. Our first objective is to determine the unknown coefficients of the excited modes in the horn to achieve the desired secant beam shape. Initially, an approximate solution is derived through analytical calculations. Given a horn with aperture size a and flare angle α_0, and considering structural symmetry, the radiated E_z field in the xy-plane can be expressed as [9]

$$E_z(\phi) = \int_{-a/2}^{a/2} F(x) e^{-jk_x x} dx \tag{1}$$

where $k_x = k \sin\phi$; $k = 2\pi/\lambda_0$; $F(x)$ represents the aperture distribution of the electric field component $E_z(x)$ as a superposition of the modal fields:

$$F(x) = \sum_m |C_{m0}| \cos\left(\frac{m\pi x}{a}\right) e^{-j(P_{m0}+\Delta_{m0}(x))}. \tag{2}$$

Here, C_{m0} are unknown modal amplitude coefficients of the aperture field; $m = 1, 3, 5, ...$ is the modal index. P_{m0} denotes the accumulated phase of each mode, while $\Delta_{m0}(x)$ quantifies the phase error at the aperture. As waves propagate radially, the phase fronts adopt a cylindrical shape, introducing path difference relative to an ideal plane wave at the aperture. At any aperture point x, the path difference, denoted as $\delta(x)$, can be determined by

$$\delta(x) = \sqrt{x^2 + L^2} - L, 0 \leq |x| \leq a/2 \tag{3}$$

where L represents the radius of curvature of the cylindrical wavefront at the aperture, as depicted in Fig. 2. For each mode, the corresponding phase error at the aperture is given by

$$\Delta_{m0}(x) = \frac{2\pi\delta(x)}{\lambda_{gm}} \tag{4}$$

where λ_{gm} represents guided wavelengths for TE_{m0} modes, defined as

$$\lambda_{gm} = \frac{\lambda_0}{\sqrt{1 - \left(\frac{m\lambda_0}{2a}\right)^2}} \tag{5}$$

To achieve the optimal beam shape, specifically, a secant distribution, the mode coefficients C_{m0} and P_{m0} are determined by satisfying the following conditions for the normalized PPW field $\overline{E_z}$

$$\overline{E_z}(\phi) = \frac{\sec(\phi/2)}{\sec(\phi_e/2)}, \quad |\phi| \leq \phi_e, \tag{6}$$

$$\overline{E_z}(\phi) < -10\,\mathrm{dB}, \quad |\phi| > \phi_e. \tag{7}$$

Here, ϕ_e represents the half-subtended angle of the sub-reflector. Eq. (6) ensures that the E_z field distribution matches the ideal pattern within the subtended angle, while Eq. (7) imposes a constraint for spillover loss outside this range. An optimization process implemented in MATLAB provides initial estimates for C_{m0} and P_{m0} at the center frequency of 90 GHz. The MHF geometry is then optimized through full-wave simulations to achieve the desired performance. The structure consists of a stepped WG with two ports [see the inset in Fig. 3 (a)]. The input port is excited with the TE_{10} mode, while the output port supports multiple higher-order modes. The S-parameters are analyzed to determine the relative amplitudes and phases for each mode of the output WG.

Initially, a dual-mode horn is considered, in which TE_{10} and TE_{30} modes dominate the modal content. In this setup, the horn aperture must satisfy $a \leq 2.5\lambda_0$ to prevent the excitation of higher-order modes, considering the short horn with a large flared angle. The approximate method predicts an optimal ratio of $|C_{30}/C_{10}|^2 \approx 0.64$, however, the full-wave simulations reveal that this ratio cannot be reached within the given aperture constraint. To provide greater flexibility in modal control, the excitation the TE_{50} is required. The optimal modal coefficients at 90 GHz for three modes are estimated as $|C_{50} : C_{30} : C_{10}|^2 \approx 0.2 : 1 : 0.66$ with corresponding phases $P_{50} \approx 99°$, $P_{30} \approx 11°$, and $P_{10} \approx 0°$. Fig. 3 (a) shows the computed power of the three modes at the output port. At 90 GHz, the full-wave results yield $|C_{50} : C_{30} : C_{10}|^2 \approx 0.25 : 1 : 0.8$, reasonably close to the predicted values. However, precisely controlling both the amplitude and phase of the three modes remains challenging. Note that in a multimode horn, modal interference at the aperture influences the final phase distribution, leading to an equivalent phase center that may deviate from the geometrical curvature center. Therefore, the lengths L_1, L_2, and L_3 are

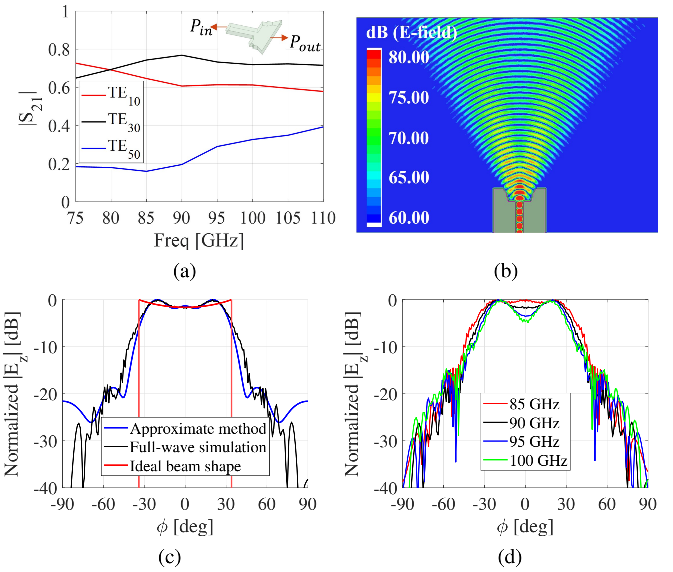

Fig. 3. (a) Computed magnitude of the transmission coefficient for the three modes. (b) Modulus of the instantaneous E-field distribution (in dB) inside the PPW at 90 GHz. (c) Comparison of the simulated $\overline{E_z}$ field distribution along the arc of the proposed MHF in the PPW at 90 GHz. (d) Full-wave simulated $\overline{E_z}$ field distribution along the arc at 85, 90, 95, and 100 GHz. Design parameters (in mm): $a_0 = 2.54, a_1 = 8, a_2 = 8.8, a = 11.67, L_1 = 1.13, L_2 = 1.15, L_3 = 1.7$.

carefully optimized through full-wave simulations to correct the phase center of the MHF.

The E-field amplitude distribution inside the PPW at 90 GHz is shown in Fig. 3 (b). Fig. 3 (c) presents the full-wave simulated $\overline{E_z}$ field distribution at 90 GHz along the arc [see Fig. 1 (b)], compared with the results from the approximate method and the ideal beam shape. The result indicates that the proposed MHF yields the sub-reflector tapering level of $-6\,$dB within a subtended angle of $2\phi_e = 68°$, considering the trade-off between high taper efficiency and low spillover loss. This behavior is consistent across a wide frequency range, as demonstrated in Fig. 3 (d).

Fig. 4 (a) shows the configuration of the entire antenna system in aluminum, which consists of the offset dual-reflector system illuminated by the proposed MHF in the PPW, and a flare towards the radiating aperture. Fig. 4 (b) compares the E-field amplitude distribution in the dual-reflector system for the proposed MHF and the original horn feed, showing a notable improvement in aperture field uniformity. The proposed MHF enhances sub-reflector taper efficiency to 97%, compared to 75% for the original horn, while incurring a 10% increase in spillover loss at 90 GHz. However, this increased spillover loss causes multiple sidewall reflections that result in phase aberrations in the optical system. To mitigate these effects, an absorber is strategically placed at a strong reflection region, effectively reducing phase variations to $\pm 15°$, as demonstrated in Fig. 4 (c). A gain improvement of $0.7\,$dBi is achieved at 90 GHz, corresponding to a 10% increase in antenna aperture efficiency. This improvement is consistently observed across the entire W-band, as shown in Fig. 4 (d). These results confirm the validity of the proposed

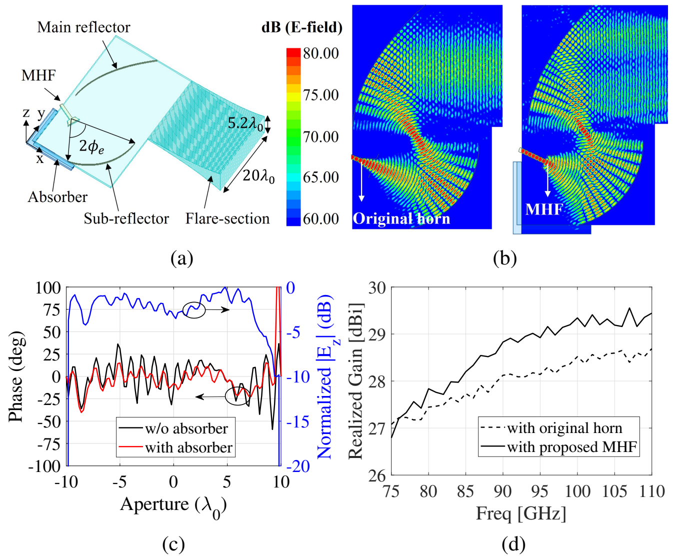

Fig. 4. (a) Configuration of the entire antenna system with the proposed MHF. (b) E-field distribution in the xy-plane at 90 GHz. (c) Amplitude and phase distribution at the main reflector aperture at 90 GHz. (d) Simulated broadside gain as a function of frequency.

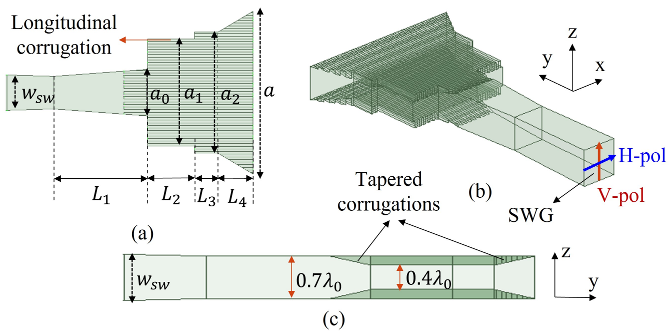

Fig. 5. Geometry of the proposed DP-MHF. (a) Top-view, (b) perspective view, and (c) side-view. Values of the design parameters (in mm): $w_{sw} = 2.54, a_0 = 8, a_1 = 8, a_2 = 9, a = 11.67, L_1 = 6.6, L_2 = 3.33, L_3 = 1.65, L_4 = 1.65$.

design and its efficiency improvement for the single-polarized configuration. The design concept is further explored to develop the dual-polarized multimode horn feed (DP-MHF), which is discussed in the following section.

III. Dual-Polarized Multimode Horn Feed

The geometry of the DP-MHF is shown in Fig. 5. Details of the corrugated feed horn can be found in [5]; the key difference in this design is the incorporation of the 2-step WG structure. For V-pol excitation, the structure closely resembles the single-polarized MHF, as the longitudinally corrugated plate performs as PEC for this polarization [5]. The design process begins by achieving the optimal modal content predicted in Section II for V-pol. Given the aperture size $a = 3.5\lambda_0$, the horn supports the TE_{01} and TE_{21} modes for H-pol excitation. However, directly controlling the modal content for H-pol is challenging, as the horn dimensions are primarily tailored to support the desired modal field for V-pol. This constraint limits the ability to precisely shape the H-pol beam. To suppress the undesired E-field spreading

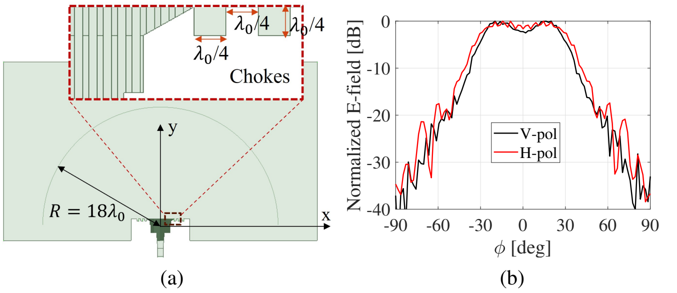

Fig. 6. (a) Configuration of the DP-MHF in PPW. (b) Simulated $\overline{E_z}$ field distribution along the arc at 90 GHz for both polarizations.

within the PPW for H-polarization, which results from strong edge diffraction due to the abrupt boundary transition at the horn aperture, several chokes have been integrated near the aperture, as shown in Fig.6 (a). With a height of approximately $0.25\lambda_0$, these chokes act as a soft surface for H-pol, effectively suppressing surface waves along the aperture metal sidewalls. The simulated $\overline{E_z}$ field distribution at 90 GHz along the arc is plotted for both polarizations in Fig. 6 (b). As seen, the H-pol beam exhibits a broader beamwidth, which consequently results in higher spillover loss.

Fig. 7 (a) illustrates the configuration of the entire antenna system with the DP-MHF, which maintains the same size as the design in [5]. To mitigate multi-reflection effects caused by increased spillover loss, absorbers have been introduced. The E-field distribution, shown in Fig.7 (c), clearly demonstrates more uniform aperture illumination for both polarizations at 90 GHz. Radiation patterns in the xy-plane at 90 GHz for two polarizations are presented in Fig. 7 (b). Higher SLLs are expected as a result of improved uniformity of the aperture field. While directivity improves by 0.4–0.8 dB across 85–110 GHz for both polarizations, gain enhancement remains limited due to increased spillover loss and the presence of absorbers.

IV. Conclusion

The design concept of MHF in the PPW is successfully validated in a single-polarized system, demonstrating a 10% improvement in aperture efficiency over 30% fractional bandwidth. While adding the absorber can effectively mitigate phase aberrations, further reduction of spillover loss requires a more precise analysis to determine the ideal modal content. In the dual-polarized configuration, increased spillover loss imposes constraints, and the limited control over the modal content for H-polarization remains a challenge. Future research could explore techniques to shape the reflector rims and minimize strong multiple reflections in targeted areas.

Acknowledgment

This work has been supported by the European Union through European Regional Development Fund (ERDF), Ministry of Higher Education and Research, CNRS, Brittany region, Conseils Départementaux d'Ille-et-Vilaine and Côtes d'Armor, Rennes Métropole, and Lannion Trégor Communauté, through the CPER Projects CyMoCod and PhotBreizh.

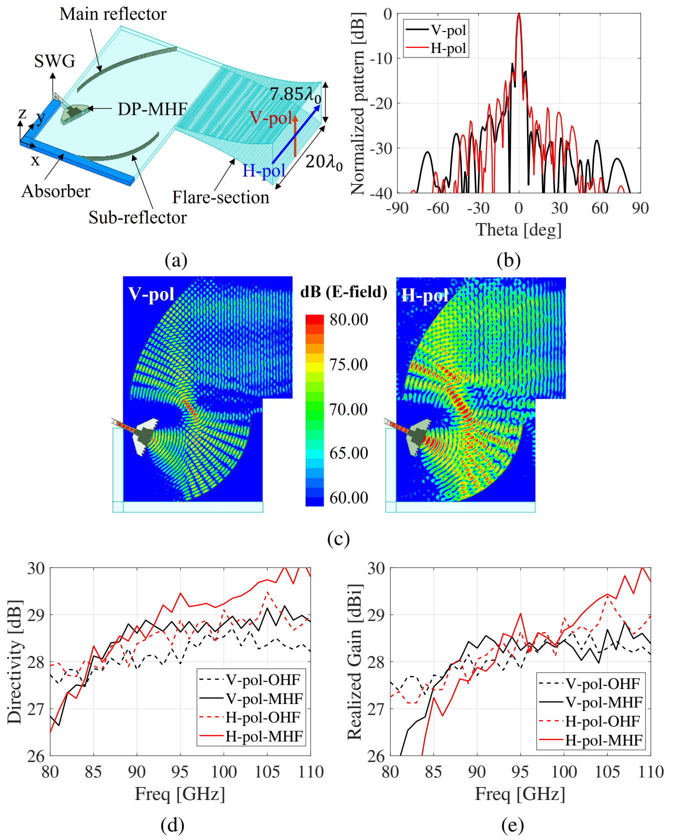

Fig. 7. (a) Overall antenna system with the DP-MHF. (b) Radiation patterns in the xy-plane of the antenna at 90 GHz. (c) E-field distribution in the offset dual-reflector system at 90 GHz. The directivity (d) and gain (e) of the antenna system are compared with those of the system using the original horn (OHF).

References

[1] D. Telekom, Cosmote, and Ericsson, "Look beyond 100 GHz to boost 5G backhaul capacity," *Ericsson News*, 2021, [Online]. Available: https://www.ericsson.com/en/news/2021/4/ericsson-trials-w-band-as-5g-backhaul-spectrum.

[2] M. Ivashina, A. Vilenskiy, H.-T. Chou, J. Oberhammer, and M. N. Mou Kehn, "Antenna technologies for beyond-5G wireless communication: Challenges and opportunities," in *Proc. Int. Symp. Antennas Propag. (ISAP)*, 2021, pp. 1–2.

[3] Y. Zhang, A. R. Vilenskiy, V. I. Litun, and M. V. Ivashina, "A W-band quasi-optical array antenna feeding network with high taper efficiency using optimal ridge excitation of an h-plane sectoral waveguide," *IEEE Antennas Wirel. Propag. Lett.*, vol. 23, no. 9, pp. 2668–2672, 2024.

[4] Y. J. Guo, M. Ansari, R. W. Ziolkowski, and N. J. G. Fonseca, "Quasi-optical multi-beam antenna technologies for B5G and 6G mmwave and THz networks: A review," *IEEE Open J. Antennas Propag.*, vol. 2, pp. 807–830, 2021.

[5] T.-K.-N. Nguyen, J. Taillieu, D. González-Ovejero, and R. Sauleau, "Low-profile and broadband dual-linearly polarized offset dual-reflector antenna for W-band applications," *IEEE Trans. Antennas Propag.*, vol. 72, no. 11, pp. 8858–8863, 2024.

[6] P. D. Potter, "A new horn antenna with suppressed sidelobes and equal beamwidths," *Microwave Journal*, vol. 6, pp. 71–78, 1963.

[7] K. Lee and R.-S. Chu, "Design and analysis of a multimode feed horn for a monopulse feed," *IEEE Trans. Antennas Propag.*, vol. 36, no. 2, pp. 171–181, 1988.

[8] C. R. Scott, "Modern methods of reflector antenna analysis and design," in Norwood, MA, USA: Artech House, 1990, ch. 8, ISBN: 978-0-89006-419-1.

[9] P.-S. Kildal, *Foundations of Antenna Engineering: A Unified Approach for Line-of-Sight and Multipath*. Norwood, MA, USA: Artech House, 2015, ISBN: 978-1-60807-868-4.